EJECTOR POWERED PROPULSION AND HIGH LIFT SUBSONIC WING

R. A. Squyers and J. L. Porter
Vought Corporation Advanced Technology Center, Dallas, Texas

K. S. Nagaraja[+] and G. F. Cudahy[*]
[+]Air Force Wright Aero Labs, Wright Patterson AFB, Ohio
[*]Fairchild Republic Corp., Long Island, N.Y.

Abstract

Methodologies based on three-dimensional vortex-lattice and lifting-line theories and two-dimensional analog techniques were coupled with viscous flow predictions and empirically-based ejector augmentor design and performance procedures to establish the design of a high performance ejector wing. As part of the design study, various ejector wing configurations were considered analytically. Superior lift and thrust performance particularly at high angles of attack were predicted for a configuration consisting of a constant-pressure mixing ejector with a lower surface inlet and upper trailing edge exhaust flow. This configuration was subsequently built and tested. Tests were conducted statically and at Mach numbers up to M_0 = .3, for a three-dimensional, swept, four ejector bay configuration and compared with a corresponding clean wing tested during the same tunnel entry. The test results indicate improvements in $(L/D)_{max}$ of up to 27 percent for the ejector wing when compared with the clean wing and an increased angle of attack capability of $\Delta\alpha > 10^o$ without stall. The ejector augmentor, although designed to improve wing performance rather than provide thrust augmentation, provided a thrust augmentation ratio $\phi = 1.06$ at the M_0 = .294 condition, as predicted in the design studies.

Nomenclature

A_3	Diffuser Inlet Area
A_4	Diffuser Exit Area
A_s/A_p	Inlet Area Ratio
A_p	Primary Inlet Flow Area
A_s	Secondary Inlet Flow Area
A	Area
AR	Aspect Ratio
BLC	Boundary Layer Control
C_D	Total Drag Coefficient
C_L	Total Lift Coefficient
C_N	Section Normal Force Coefficient
C_d	Section Drag Coefficient
C_j	Total Jet Momentum Coefficient
C_ℓ	Section Lift Coefficient
C_p	Local Pressure Coefficient
D	Drag
F	Thrust
L	Lift
M	Mach Number
NPR	Nozzle Pressure Ratio
$\dot{m}$	Mass Flow Rate
P	Pressure
P_{s_i}	Secondary Inlet Static Pressure
PR	Pressure Ratio, P_{t_p}/P_{t_s}
S	Wing Area
T_{t_p}	Primary Fluid Total Temperature
T_{t_s}	Secondary Fluid Total Temperature
TR	Total Temperature Ratio
U, V	Velocity
c	Airfoil Chord Length
q	Dynamic Pressure
x	Axial Distance
α	Geometric Angle of Attack
β	Entrainment ratio, $\dot{m}_s/\dot{m}_p$
γ	Ratio of Specific Heats
ϕ	Thrust Augmentation Ratio

Subscripts

1	Mixing Region
2	Throat
3	Diffuser Entrance
4	Diffuser Exit
j	Blowing Jet Condition
amb, 0	Freestream Condition
e, ex	Exit Location
ej	Ejector
i, ideal	For Expansion to Ambient Static Pressure
isen	Isentropic
max	Maximum
net	Net, (Gross Thrust Minus Ram Drag)
p	Primary Flow Condition
ref	Reference
t	Total Condition

Superscripts

'	Isentropically Expanded to Ambient Pressure
*	Sonic Condition

1.0 INTRODUCTION

The use of ejector augmentors for flight vehicles has had but limited success in the past. Some feasibility was previously demonstrated by such attempts as the Boeing/DeHavilland "Buffalo", the Lockheed "Hummingbird", and more recently, the Rockwell XFV-12A and the Ball-Bartoe "Jet Wing" aircraft. With the exception of the XFV-12A, all of these vehicles have flown more or less successfully. On the other hand, the performance characteristics of both the Boeing YC-14 and the McDonnell-Douglas YC-15, which use non-ejector propulsive lift augmentation (upper surface and under the wing blowing, respectively), appeared exceptionally good. It thus appears that the proper use of propulsion system exhaust for an ejector wing hinges on the correct design of the ejector augmentor and the proper integration of the ejector's geometric and operating characteristics with the wing geometric and aerodynamic characteristics. No explicit theories for the "correct" design of the ejector augmentor, as pointed out in reference (2), currently exist. For instance, while the recent theory indicates that devices with constant pressure mixing and supersonic mixed flow may result in significantly better ejector performance at forward flight conditions than constant area mixing with subsonic mixed flow, virtually no experimental information to validate this is available. Furthermore, the type of mixing and the resulting secondary flow entrainment and jet exhaust significantly interact with the three-dimensional wing aerodynamic performance in such a complex way that no current theories are capable of optimizing an integrated system design.

Despite the foregoing difficulties, the benefits of an ejector wing aircraft in terms of higher propulsive efficiency, enhanced lift, maneuvering capability and quietness were significant enough to warrant the effort to achieve a viable design.

The objectives of this program were (1) to develop an ejector analytical procedure which would be appropriate to establishing the theoretical ejector/wing aerodynamics, and which would provide insight into the key parameters to be investigated experimentally, and (2) to design and test a parametric three-dimensional model which would provide data relevant to achieving a capability for designing a functional high performance ejector/wing subject to aircraft constraints.

2.0 ANALYSIS AND DESIGN

The approach of the analysis consisted of using existing methods of ejector anlayses to define the best type of ejector to be used, and the critical geometric and flow parameters. Analytical ejector results were then combined with existing techniques of two and three dimensional wing analyses to arrive at ejector/wing aerodynamics, and the definition of the parametric three-dimensional model.

2.1 Ejector Performance Analysis

Ejector analyses were formulated and exercised for "isolated" (i.e., not yet integrated into a wing) ejectors, in order to establish the most appropriate ejector to be used. The effects of parameters which are critical to ejector performance were analytically examined in this task. The parameters which are most critical are the following:

- Geometric
  1. Secondary and Primary Inlet Area Ratio
  2. Mixing Section to Primary Area Ratio
  3. Diffuser Area Ratio
  4. Mixing Section Length

- Fluid Properties
  1. Primary to Secondary Total Pressure Ratio
  2. Primary to Secondary Total Temperature Ratio
  3. Primary to Secondary Gas Constant and Specific Heat Ratios
  4. Mixing Plane Static Pressure
  5. Primary to Secondary Mach Number or Velocity Ratio

- Loss Mechanisms
  1. Secondary Inlet Flow Velocity Non-Uniformity
  2. Skin Friction Losses/Separation Effects
  3. Shock Losses
  4. Incomplete Mixing Losses
  5. Exit Flow Skewness
  6. Three-Dimensional Installation Losses

Ejector performance for a constant pressure mixing device provided performance preditions, including mixed flow solutions. Analytical results for the constant pressure device were compared with analytical results from a computer program which predicts performance for a constant area mixing device. Both programs included comparable effects of losses such as those arising from: incomplete mixing, skin friction, reduced diffuser efficiency, etc. The comparisons included effects of geometric variations, secondary fluid conditions corresponding to different flight conditions, and primary fluid conditions corresponding to real engine bypass or bleed conditions. The latter information enabled selection of the primary air source characteristics to be used during the experimental testing. From these comparisons, the best ejector type was selected, based on thrust performance for varying flight conditions, as well as geometric suitability to airfoil integration.

Computational codes for constant area and constant pressure mixing were modified to enable the ejector exit static pressure boundary condition to be specified. The effect of local pressures caused by the wing flow field was assessed in terms of influence on ejector performance. Modifications enabling the ejector mixed exit flow to exhaust supersonically were also made for comparison with conventional analysis in which supersonic mixed flow undergoes a transverse normal shock before exiting subsonically. The codes provided parametric performance information in terms of augmentation ratio and entrainment ratio as a function of inlet and diffuser area ratios for specified primary and secondary gas properties (total pressure, total temperature, etc.). The effects of forward flight on the ejector-alone gross and net thrust were determined.

A variety of ejector configurations, for varying primary and secondary stagnation conditions were investigated analytically. For both constant area and constant pressure mixing ejectors, subsonic and supersonic mixed flows solutions were investigated by increasing the primary nozzle exit Mach number which lowers the mixing plane entrance static pressure and increases the secondary flow Mach number. For the supersonic solutions, various exhaust conditions were assumed, as follows: (a) Supersonic mixed flow with no area contraction and no shock - i.e., supersonic acceleration in the exhaust diffuser/nozzle; (b) supersonic mixed flow decelerated to the minimum contraction area (corresponding to a second throat wind tunnel solution), with a shock at the minimum contraction section Mach number, followed by a subsonic nozzle; and (c) condition (b), above, but with no shock. For the cases examined, mixed flow Mach numbers were generally close to 1.0, so shock losses were minimal.

For the low secondary inlet to primary exit area ratios considered for incorporation into the wing, As/Ap = 1.0 to 10., constant pressure mixing providing better ejector preformance than constant area mixing. Figure 1 shows a carpet plot representative of the anlaytical results obtained. It may be seen that for equivalent inlet initial conditions, the constant pressure mixing provided a higher thrust augmentation ratio at a lower exit to primary area ratio for a baseline M_0 = .15 case.

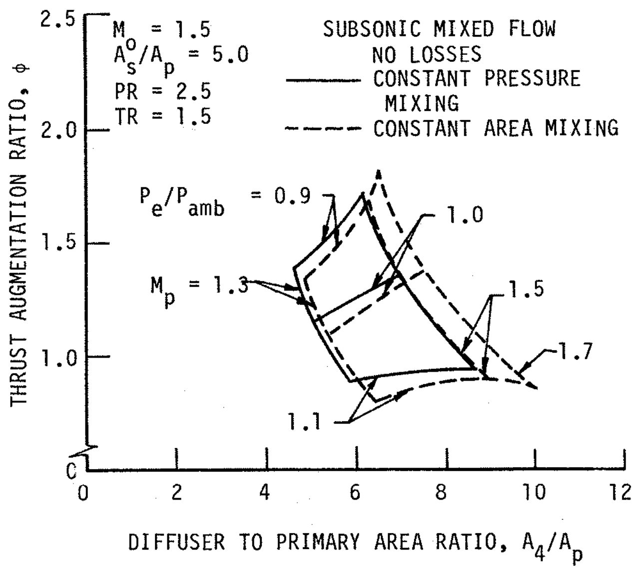

FIGURE 1. COMPARISON OF CONSTANT AREA AND CONSTANT PRESSURE MIXING PERFORMANCE FOR M_o = .15

Empirical results[1] indicate that for constant pressure mixing ejectors with a shock at the minimum contraction area, the total losses of the device can be accounted for by a 15 percent reduction in both total pressure and mass flow ratio from the theoretically predicted values corresponding to specific geometry and initial stagnation conditions. While these results have been validated by separate proprietary experimental data, several considerations for the ejector design of this study indicated significantly reduced losses. These were: (a) The mixed flow Mach number could be forced to a subsonic condition through proper design of the convergent-divergent primary nozzle. Even for supersonic mixed flow Mach numbers, shock losses were minimal because of the near-sonic condition of the viscid flow. Results of reference 1 and the proprietary experiments were all for high mixed flow Mach numbers and shocks at ~ M ≥ 2.0, (b) Boundary layer control (BLC) in the inlet and exit nozzle sections could significantly improve the entrainment and exhaust total pressure performance, as indicated in reference 2, (c) a variable diffuser area ratio, A_4/A_3, would enable near optimal conditions to be obtained, as opposed to the constant exit area tested in reference 1, and (d) at forward flight conditions, the Configuration C shown in Figure 2 would have a "ram momentum" component in the lift direction, reducing the ram drag term.

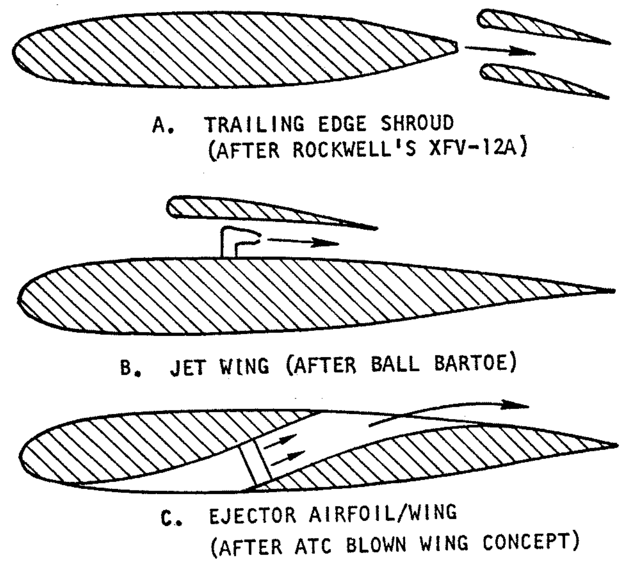

FIGURE 2. CANDIDATE EJECTOR/WING CONFIGURATIONS

Reductions in ejector performance corresponding to (a) a 15 percent reduction in both mass flow ratio, β, and exit total pressure, p_{te}, and (b) a 7.5 percent reduction in β and p_{te}, were considered. The 7.5 percent reduction cases were considered to represent low risk, reasonable performance predictions, while the 15 percent reductions represented "worst case" performance. The results of these analyses for constant pressure mixing are presented in Figure 3. In this figure the "worst case" results show virtually no thrust augmentation, even statically, and at the M_0 = .3 condition, augmentation ratios less than 1.0 are indicated. The augmentation ratio definition being used for the forward flight conditions compares the ejector net thrust with the ideal primary net thrust, i.e., a ram drag penalty for the ideal primary thrust has been used. This form of the thrust augmentation ratio is given below:

$$\phi = \frac{F_{gross\ ejector} - (\dot{m}_s + \dot{m}_p)\ V_o}{\dot{m}_p\ (V_p' - V_o)} \quad (1)$$

where the ideal primary net thrust is:

$$F_p' = \dot{m}_p(V_p' - V_o) \quad (2)$$

An interesting result shown in Figure 3 for the "worst case" losses is the inlet area ratio crossover with increasing M_o. While this possibility was described by von Ohain,[2] it is not predicted by the loss-free results, or for the 7.5 percent losses results. It is, however, a significant result and indicates that the capability of varying inlet area ratio to optimize performance at forward flight condition is desirable. The possibility of varying the primary nozzle exit plane location relative to the converging secondary inlet section was therefore considered for the experimental model.

The 7.5 percent losses results shown in Figure 3 indicate reasonably high augmentation ratios statically, and values slightly greater than ϕ = 1.0 at the M = .3 condition. Ejector performance of this type represented a low risk design capable of providing a high L/D for the ejector wing.

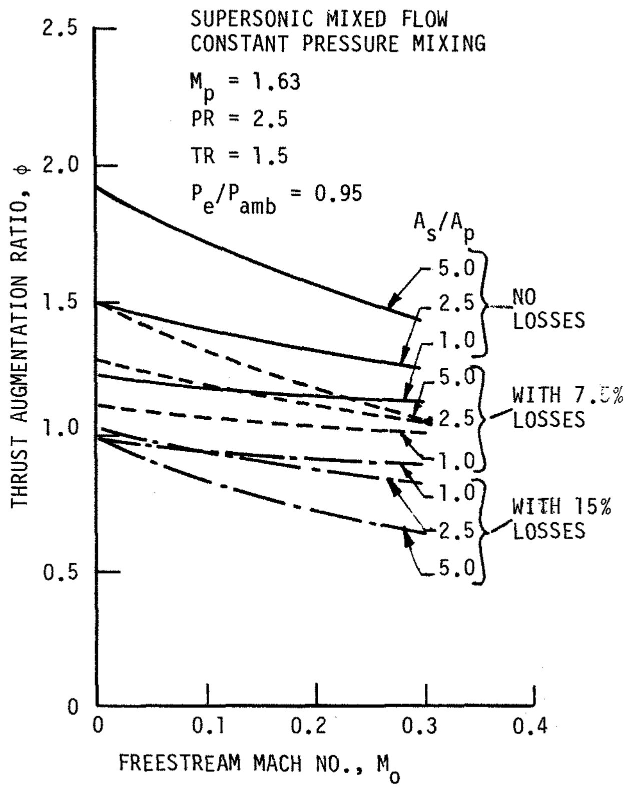

FIGURE 3. EFFECTS OF LOSSES ON EJECTOR AUGMENTATION RATIO VS M_o

2.2 Ejector/Wing Aerodynamics Analysis

In-house wing aerodynamic codes for lifting-line and jet-flap vortex lattice analyses were modified to accept output from the ejector-alone codes. Ejector code jet exit specifications were used as "jet flap" input data for the wind analyses. The evaluation of the "isolated" ejector performance was supplemented by consideration of the following effects:

- Integration of an ejector with a three-dimensional wing
- Subsonic flight Mach Numbers and angles of attack

Analytical results for the isolated ejector were used to provide input to a modified thin wing/jet vortex lattice computer code,[3] for airfoil analysis. The vortex lattice method was particularly appropriate to this analytical task since the ejector secondary inflow could be represented as a "sink" on the airfoil surface, and the ejector mixed flow exhaust conditions as a "source". The vortex lattice program is part of a series of wing aerodynamic codes developed by Vought under contract to NASA-Ames covering complex flapped planforms, jet flap wings, and blown flap/jet flap analogies. It is based upon a two-element lifting surface, with a sink and source to represent the ejector inlet and exhaust mass flows, respectively, see Figure 4. Orientation of the two surface elements was arbitrary as were the strengths of the sink and source so that mass addition could be accounted for. This model was used to aid in configuration comparison and selection for the three ejector wing types shown in Figure 2. Considerable "real" flow viscous effects and forward velocity integration techniques were used on a final ranking criteria to select the ejector wing configuration.

Following initial screening through the vortex lattice analyses, use was made of proprietary multi-element analog techniques which enabled determination of detailed pressure distributions for complex two-dimensional propulsive-wing flows with finite thickness effects. These analog techniques have been extensively validated,[4,5] and permitted the inclusion of boundary layer and separation effects. They thus enabled the establishment of an ejector/wing design procedure which avoids the flow separation difficulties inherent in other treatments. The results from the predictions for two-dimensional airfoils were compared with existing data[6] to establish a baseline from which parametric incremental ejector/wing aerodynamic effects were generated.

Finally, three dimensional ejector/wing aerodynamics, including the effects of thickness, were computed using the analog information as input to an existing advanced "lifting line" program[7] based on the Weissinger "L-method".

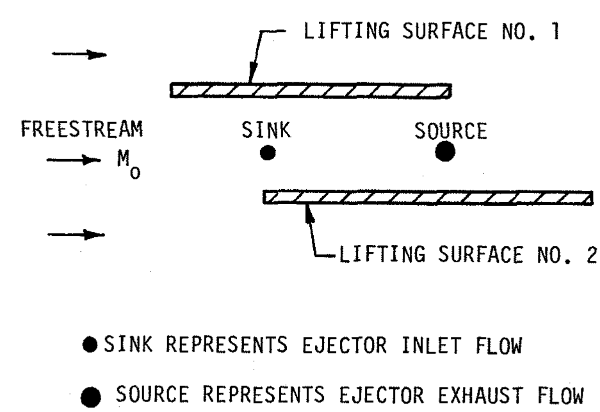

FIGURE 4. SCHEMATIC OF EJECTOR WING VORTEX LATTICE MODEL

2.3 Parametric Integrated Ejector/Wing Analysis

With the baseline ejector performance and ejector/wing aerodynamic prediction techniques established, parametric analyses to determine the configurations with significant improvements in the lift/net thrust relationship were accomplished. These parametric effects included:

- Varying ejector inlet and exhaust conditions to correspond to local wing flow conditions, and determination of the appropriate associated inlet condition.
- Varying ejector primary flow stagnation properties.
- Varying chordwise locations for the ejector inlet and exhaust flow.
- Varying freestream conditions (Mach No. and angle of attack).

Both two-dimensional and three-dimensional analyses were conducted. The results of the parametric study were used to identify the critical experimental and design parameters so that the ejector/wing model detailed design could be accomplished. The foregoing parametric studies were also used to establish the wind tunnel test plan and control range.

The coupling of the selected ejector configuration into a wing in forward flight was investigated with the use of an analog simulation facility. Figure 5 is an example of ejector wing characteristic results obtained using this facility. The streamline patterns illustrated are for an unpowered wing section at angle of attack; with ejector flow-through, but no pumping. The effects of angle of attack, total pressure coefficients and section lift coefficients were also generated in the facility. Extensive refinement of the basic airfoil external contours and the integral ejector inlet contours was accomplished through an iterative design procedure using the analog facility to predict local pressure coefficients and flow streamlines, and using these pressure predictions to perform boundary layer calculations. This iterative procedure enabled the contours to be modified during the process, to avoid flow separation.

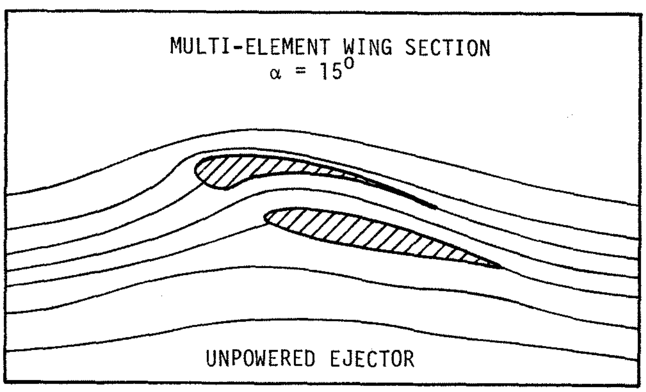

FIGURE 5. ANALOG FACILITY RESULTS FOR AN UNPOWERED EJECTOR WING

With the finalization of the airfoil contours and the corresponding prediction of two-dimensional (2-D) section characteristics, the detailed prediction of three-dimensional (3-D) ejector wing performance was possible. Figure 6 shows the 3-D theoretical prediction for lift coefficient vs. angle of attack in comparison with the 3-D non-linear performance, based on 2-D section characteristics, for the clean (no ejector wing. The corresponding drag polar (C_L vs C_D) was predicted for the clean wing.

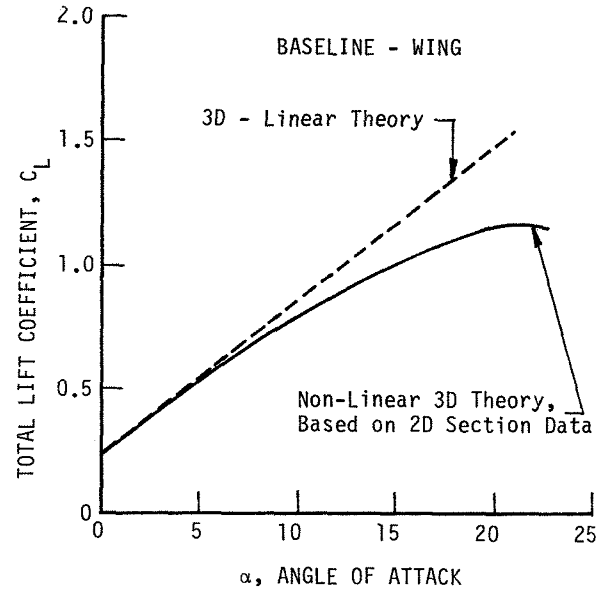

FIGURE 6. PREDICTED BASELINE WING LIFT CHARACTERISTICS

2.4 Detailed Model Design

Detailed design drawings for use in fabrication of the parametric model, permitting variations in the critical parameters identified were prepared. The designs were configured to conform in size and structural viability with the characteristics of the wind tunnel. A balance [8] was available which was particularly suitable for the ejector wing tests, since it is specially configured for supplying auxiliary air to a powered model, and for side loading (the lift direction for the ejector wing model).

In addition to the wind tunnel facility capability, basic design features for the ejector wing were addressed by consideration of the Ball-Bartoe augmentor wing aircraft, and two attack aircraft in the current USAF inventory: the A-37B and the A-7D. The relationship between the engine flow throat area (corresponding to an ejector primary throat area) and the wing geometry is summarized in Table 1. To maintain a similar relationship between the ejector primary throat area and the primary throat area and the wing area for the current design, and the maximum available auxiliary air flow indicated by reference 8 (10 lb/sec), the current half-span ejector wing could have an area, S, equal to 7.5 ft^2. For the fundamental wing geometric relationships and a leading edge sweep angle of ~7.5°, the ejector wing planform geometry was thus specified. To reduce wing tip and fuselage interference effect for the preliminary designs, the ejector primary throat area extended over only 73 percent of the semi-span model.

The mechanical design of the ejector wing wind tunnel model was then completed, incorporating as final design features all the planned geometric variations of the model and assurance of compatibility with the accessory and support structures, such as the primary nozzle system and the wind tunnel balance adaptor. The completed model

TABLE 1. SUMMARY FOR THREE EXISTING AIRCRAFT WING GEOMETRY AND ENGINE FLOW CHARACTERISTICS

AIRCRAFT	S, WING AREA, FT^2	ASPECT RATIO AR	ENGINE THROAT AREA, A^* FT^2	$A^*/\bar{c}b$	A^*/S
BALL-BARTOE	105	4.5	1.10	.0186	.0106
A-37B	184	6.2	1.672	.0155	.0091
A-7D	375	4.0	4.42	.0196	.0118
			AVERAGE →	.0179	.0105

design was also reviewed in detail to ensure compatibility with primary structure and sub-component structure fabrication. A cutaway illustration of the ejector wing model is shown in Figure 7. Section drawings taken at critical wing stations showed that the ejector bay was properly embedded in the wing structure and provided for in the stress analysis. The wing stress analysis showed the wind tunnel model to be acceptable as designed. The design assured a minimum safety factor of 5.0 on the ultimate, and 3.0 on the yield strength, of the material.

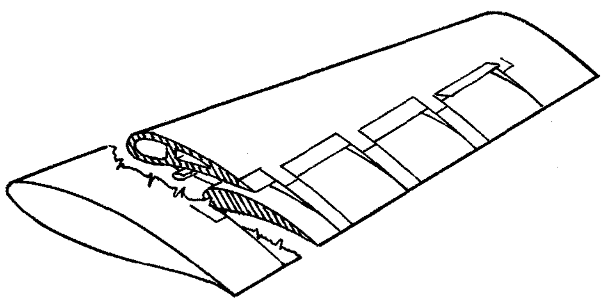

FIGURE 7. EJECTOR WING WIND TUNNEL MODEL

3.0 MODEL FABRICATION AND WIND TUNNEL TEST

3.1 Ejector Wing Model-Fabrication Techniques

The procedures for the wing fabrication and assembly included: rough cutting the bulk material, assuring the mating of the various wing and ejector subcomponent structures, and the final fabrication of several individual ejector wing parts. The machining of the ejector wing contours and plenums was accomplished primarily by Numerical Control (NC) machining, used for the final rough cut of the assembled wing model. The model finish work and detailed instrumentation were accomplished separately. The primary nozzles were manufactured from steel to enable the higher temperature primary flow conditions.

3.2 Wind Tunnel Test Plan

Concurrently with the model fabrication, details of the wind tunnel test plan were finalized and a data reduction program defined. The test plan and data reduction programs were coordinated to finalize the tunnel requirements for the ejector wing model tests. The five component strain gauge balance was first calibrated for non-blowing, static loads. The 7'x10' Wind Tunnel (No. 2) auxiliary flow system for use in powering the ejector/wing model was also calibrated. The system was found to be capable of supplying up to 8.0 lbm/sec flow at a total temperature ratio of approximately 1.35 at steady flow conditions. The blowing system was then integrated with the flow-through balance, and the balance calibration was repeated for the blowing-on conditions.

While the overall Ejector Wing performance could be obtained from the 5-component balance, the magnitude of the individual wing lift/drag components and such individual parameters as augmented thrust, vectored additional lift and secondary ram drag could only be determined with detailed integrated instrumentation, as designated in Figure 8. Such additional instrumentation, internal and external to the wing model, was incorporated into the model, and in the data reduction program. With the addition of these measurements, detailed individual ejector operation could be calculated and compared to ideal and overall measured properties.

4.0 WIND TUNNEL TEST RESULTS

The Ejector Wing model was tested in the Army Aeromechanics Laboratory 7'x10' Wind tunnel at the NASA-Ames Research center. The test matrix included a wide range of primary stagnation pressure and temperature values, representative of engine bypass bleed conditions; a range of ejector geometries, including discrete bay/part span operation; and angle of attack from -10^o to $+35^o$ for freestream Mach numbers from 0 to ~.30.

As stated earlier in this report, the philosophy underlying this Ejector Wing configuration was to achieve modest ejector thrust augmentation at the M_0 = .3 test condition, while utilizing the ejector flow conditions to significantly enhance the wing aerodynamic performance. Because of the difficulty in separating the aerodynamic and propulsive contributions, it was recognized that baseline wing, with ejector inlets and exhausts sealed, force data would be necessary in order to establish the benefits of the Ejector Wing.

Because ejector augmentation, for "conventional" ejectors falls rapidly with increased forward velocity, the ejector was designed to achieve an augmentation ratio, ϕ = 1.07, at the

M_o = .30 condition. This design goal represented approximately a 5 percent improvement over the best previously published performance for ejector augmentors at M_o = .30, as indicated by an intensive literature survey.[2] It was also believed to be a conservative estimate of achievable performance, based on empirical corrections to the analytical results.

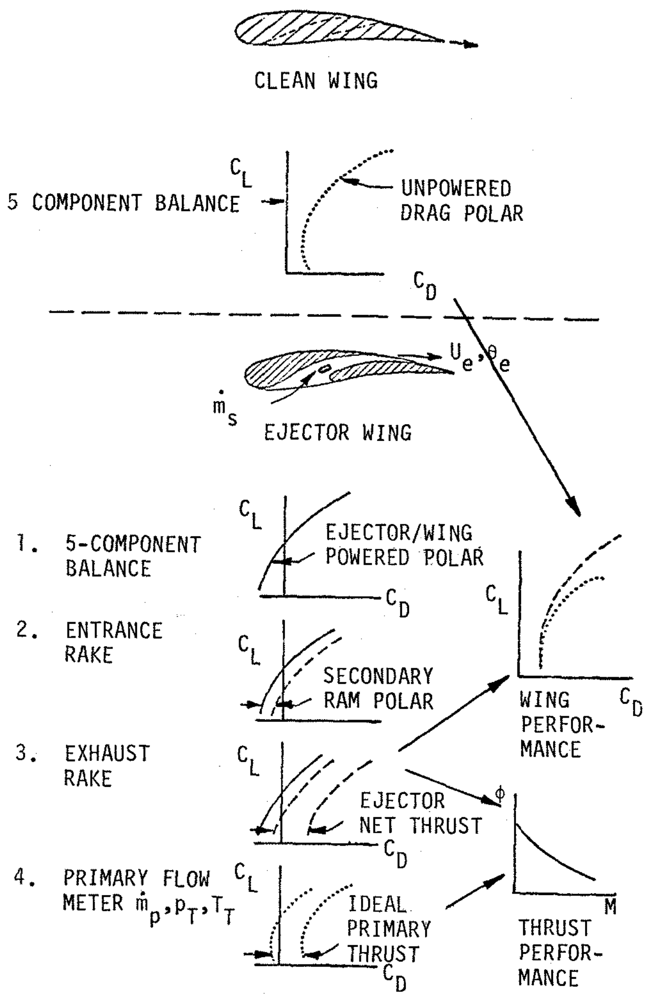

FIGURE 8. DATA REDUCTION OBJECTIVES

The objective for maximum lift coefficient, as a function of angle of attack was an improvement, ΔC_L = 1.0 over the baseline wing, and this was expected to occur at an increased incipient stall angle of attack of ~35°, vs ~15° for the baseline wing. The most significant performance objective for the Ejector Wing, however, was an increase in the maximum lift to drag ratio, (L/D)max, which would correspond to significant potential range benefits. The objective for Δ (L/D)max was a 15 percent improvement over the baseline wing powered by a "dragless nacelle" having thrust equal to the ideal thrust of the ejector primary flow. In addition to the foregoing, a secondary objective of the test was to determine maneuvering performance for partial span operation of the ejectors.

4.2 Test Results

Results of the wind tunnel tests for a variety of operating conditions are shown in Figures 9-11,

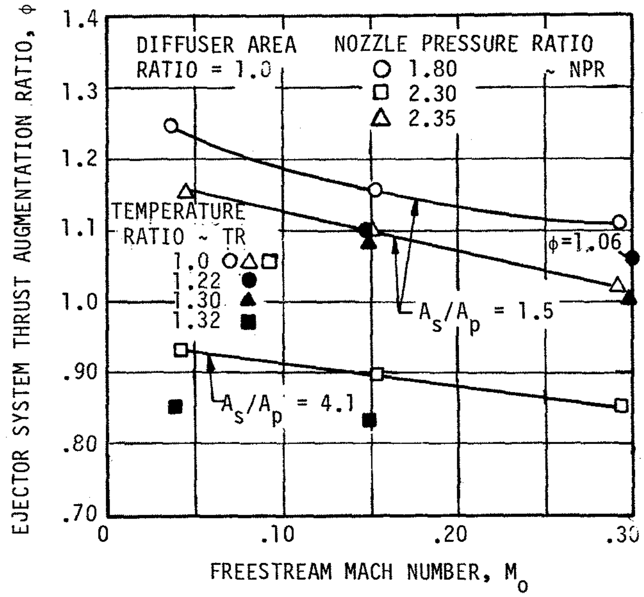

FIGURE 9. EJECTOR/WING THRUST AUGMENTATION PERFORMANCE WITH A_4/A_3 = 1.0

in terms of ejector thrust augmentation ratio vs freestream Mach Number. The predicted optimum design condition for the M_o = .3 design point was validated, as shown in Figure 9 where it may be seen that for p_{t_p}/p_{t_s} = 1.8, T_{t_p}/T_{t_s} = 1.22, and As/Ap = 1.5 an augmentation ratio of ϕ = 1.11, indicating a 10 percent improvement over the best previously published comparable results.

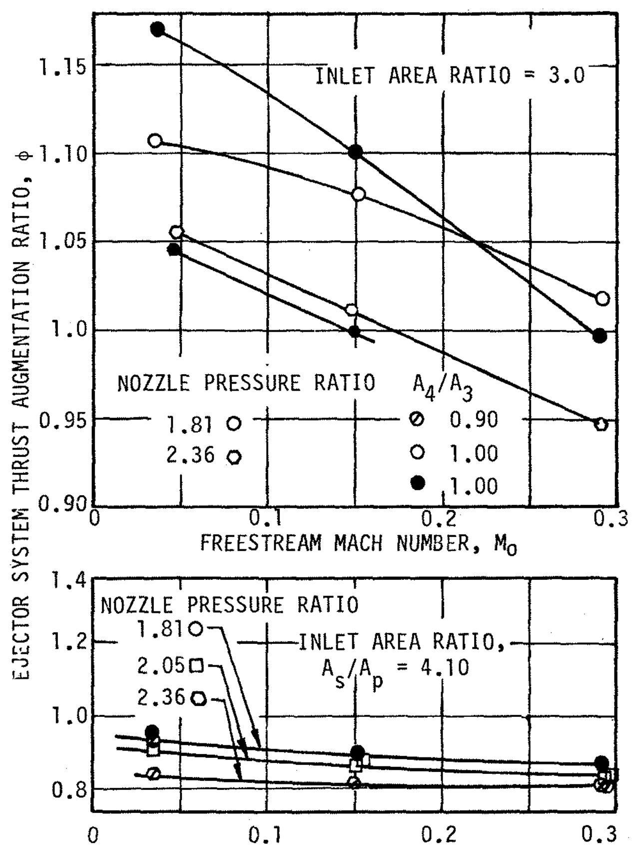

FIGURE 10. EJECTOR/WING THRUST AUGMENTATION PERFORMANCE FOR A_2/A_1 = 3.0 and 4.10

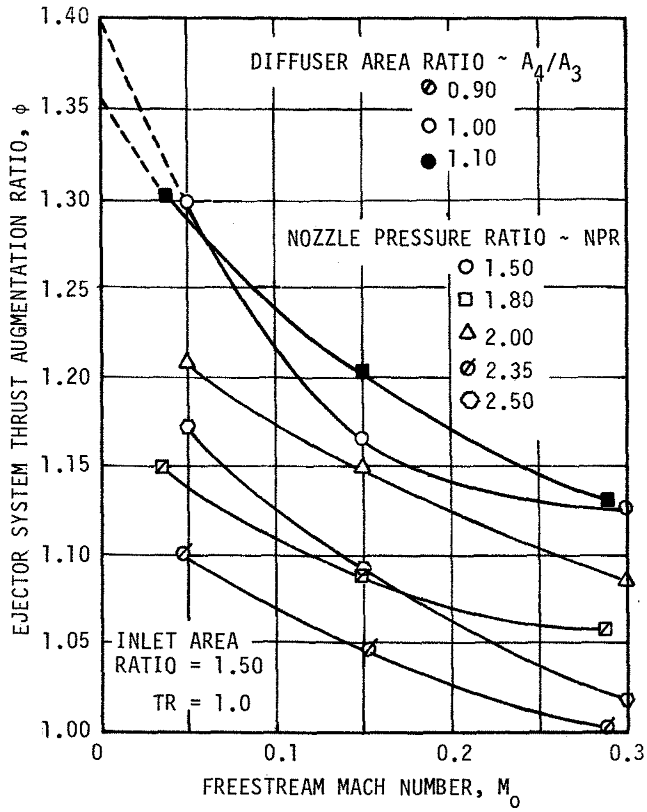

FIGURE 11. EFFECTS OF NOZZLE PRESSURE RATIO AND DIFFUSER AREA RATIO ON EJECTOR THRUST AUGMENTATION

It should be noted that the curves of ejector performance shown in Figures 9 - 11 do not have data points for the static $M_o = 0$ condition. This is because the ejector "pumped" the closed circuit wind tunnel for what would have otherwise been static operation.

Figure 12 indicates the benefits achieved by the ejector wing in terms of increased lift performance and increased maximum angle of attack for the freestream Mach number 0.15. As can be seen in Figure 12, a ΔC_L of ~ 1.20 over the baseline configuration was achieved at $\alpha = 12^o$, and was almost totally stalled at $\alpha = 22^o$; whereas the Ejector Wing continued to show good lift performance characteristics up to $\alpha = 35^o$, the maximum tunnel capability. Figure 12 also compares the Ejector and Baseline wings with estimated performance for a "jet flap" wing. As shown in the figures, the benefits of the integrated aero propulsive configuration are also significantly better than can be achieved with a comparable jet flap configuration.

The data for the Ejector Wing lift/drag relationship are presented in Figures 13 - 15 for various combinations of the parametric configurations tested. Also shown on the figures is the baseline (unpowered) configuration and the ideal primary thrust, $F_p{}'$, corresponding to each ejector operating condition. It can be seen from these figures that for each freestream Mach Number there exists an ejector geometry and operating condition which not only produces more thrust than the ideal primary jets, but also achieves significant aerodynamic benefits.

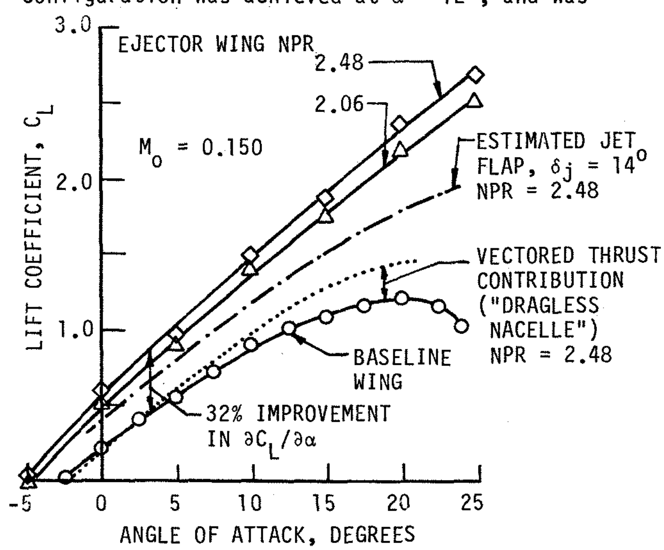

FIGURE 12. EJECTOR/WING LIFT ENHANCEMENT (SUPERCIRCULATION EFFECT) COMPARISONS

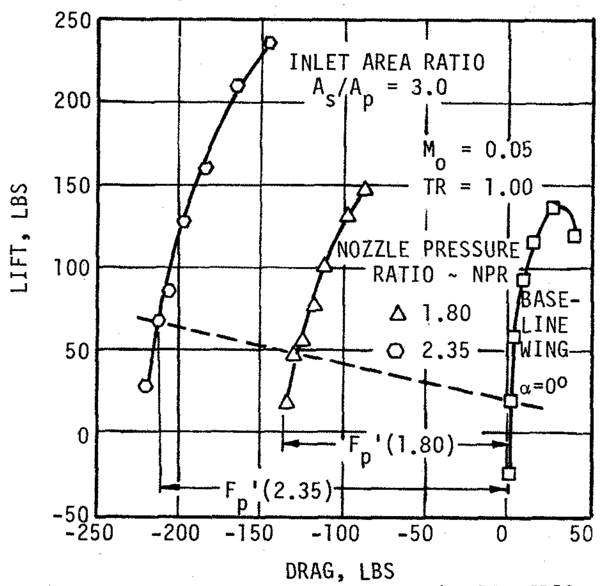

FIGURE 13. EJECTOR WING LIFT/DRAG CHARACTERISTICS WITH DIFFUSER AREA RATIO OF 1.0, @ M_o = .05, FOR A_s/A_p = 3.0

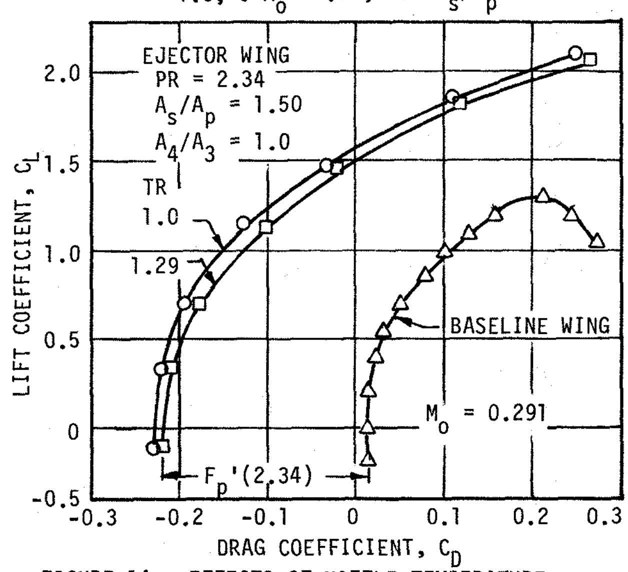

FIGURE 14. EFFECTS OF NOZZLE TEMPERATURE RATIO ON C_L, C_D PERFORMANCE

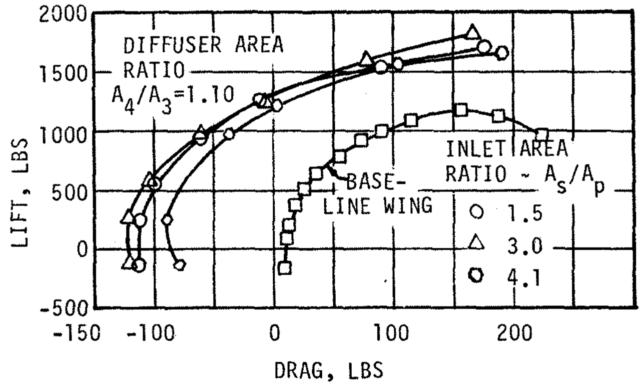

FIGURE 15. EJECTOR WING LIFT/DRAG CHARACTERISTICS WITH DIFFUSER AREA RATIO OF 1.10 @ M_o = 0.29, FOR VARIOUS A_s/A_p's

Figure 16 illustrates these aerodynamic performance benefits more conclusively, by eliminating the direct propulsive vectoring contributions for the Ejector Wing, and comparing the result with the baseline wing aerodynamic performance. As seen in the figure, the enhancement of the external flow (aerodynamic) conditions by the ejector operation resulted in lower wing drag at a given value of lift coefficient, or a higher lift at a specified drag coefficient. The super-circulation effect was observed in the smoke-flow streamline characteristics generated during the test.

The results shown in Figure 16 indicate an improvement in the maximum lift/drag ratio, (L/D)max, of 27 percent over the baseline wing. From the Brequet range equation, this would translate directly into a 27 percent improvement in range. A further improvement in overall performance would accrue from the improvement in propulsive specific fuel consumption (not accounted for in Figure 16) due to the ejector thrust augmentation. Improvements in maneuvering capability are also indicated by results similar to those shown in Figure 16 by the continuation of the lift/drag polar to very high values of C_L without any appreciable decrease in lift at very high drag values.

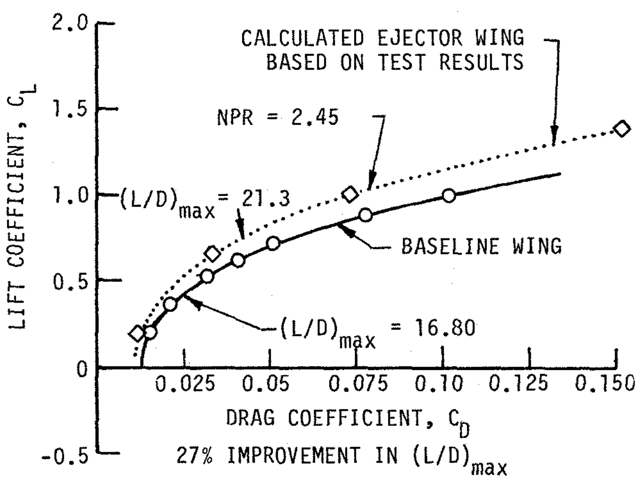

FIGURE 16. AERODYNAMIC PERFORMANCE COMPARISON WITHOUT POWER EFFECTS

The potential of the Ejector Wing to achieve high roll rates was also considered in the testing, by examination of performance with two inboard ejector bays sealed off (inlet and exit). In Figure 17 the rolling moment for the Ejector Wing with all four bays operating is compared to that with the inboard bays sealed off. As can be seen in the figure, very high rolling moments can be achieved in this manner at equivalent lift coefficients. The vectoring of the thrust at the wing trailing edge contributes to the rolling moment and is comparable to an augmented wing-tip thrust vector control.

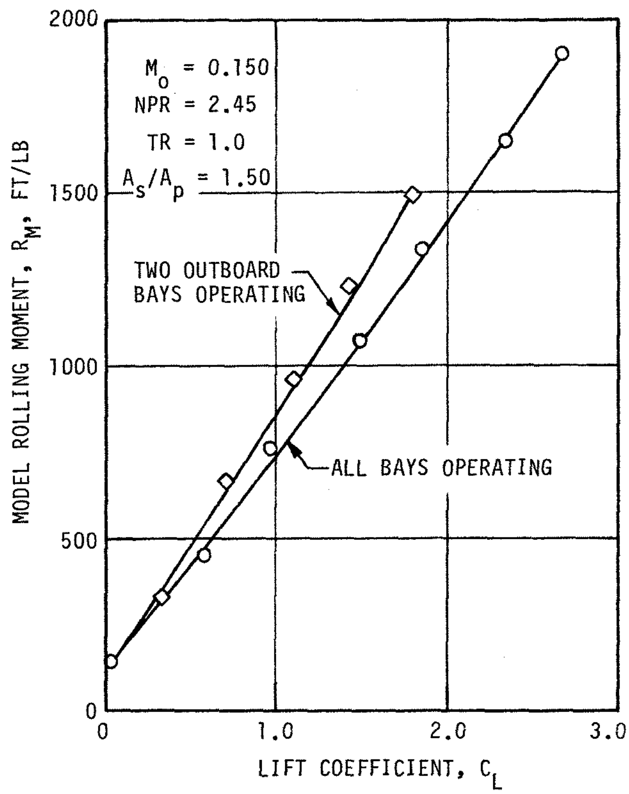

FIGURE 17. EFFECTS OF PARTIAL SPAN EJECTOR OPERATION ON MANEUVERING ROLLING MOMENT

4.3 Comparison of Test Results with Analytical Predictions

As can be inferred from the previous sections, the test results in general met or surpassed the objectives set for the Ejector Wing. In the following paragraphs, the test data are compared with analytical predictions. Figure 18 shows the ejector thrust augmentation test data for the predicted best geometric configuration in comparison with the analytic predictions made prior to the test. As can be seen in the figure, the augmentation ratio was exceeded at M_O = .3 for the temperature ratio TR = 1.0 case, and almost identically matched for the TR = 1.22 case in Figure 9.

At static conditions, higher augmentation ratios than predicted analytically were achieved during testing. The C_L vs α curves shown in Figure 19 for the baseline and Ejector Wing test data and analytic predictions again indicate that the analytical procedures used for the Phase I tasks are both valid and accurate.

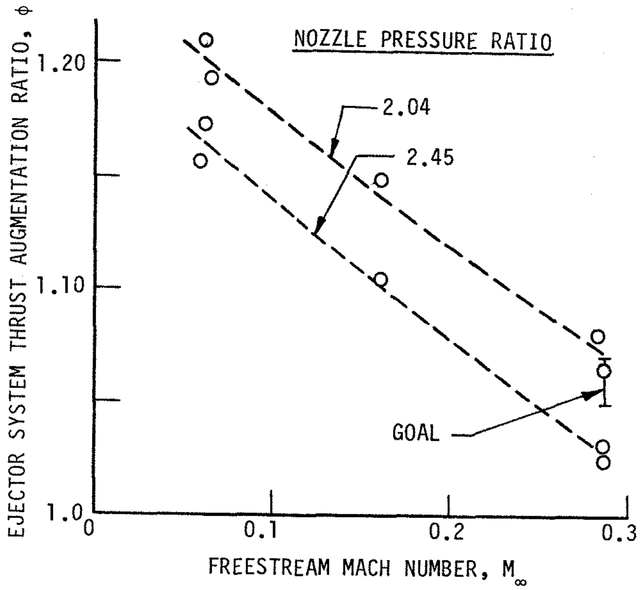

FIGURE 18. EJECTOR SYSTEM PERFORMANCE AS A FUNCTION OF M_0 AND NPR

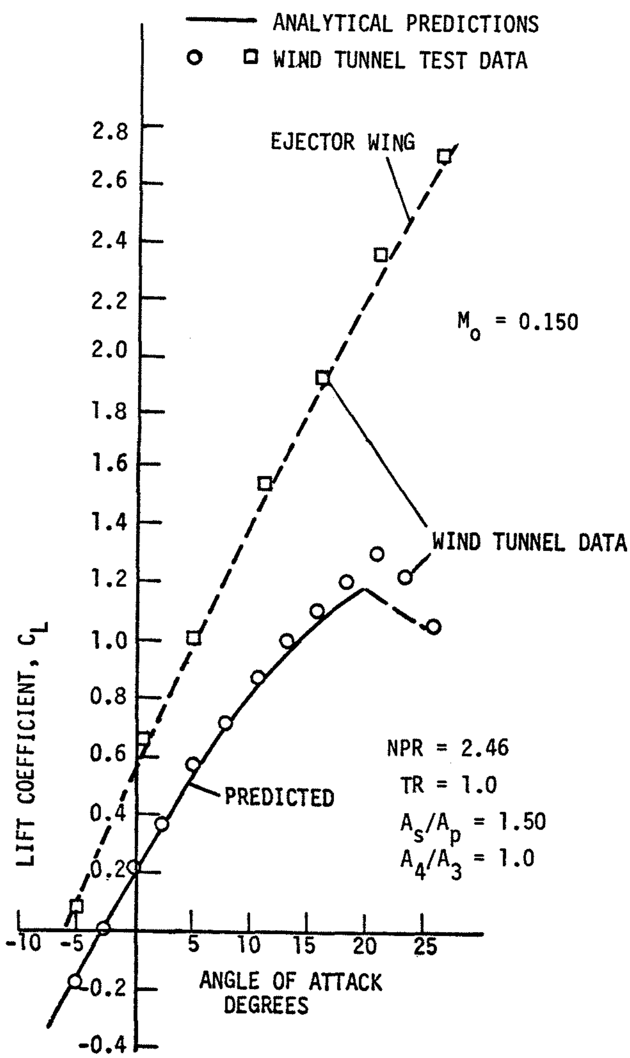

FIGURE 19. COMPARISONS OF BASELINE AND EJECTOR WING LIFTING PERFORMANCE AND PREDICTED RESULTS

In Figure 20 the analytical drag polars for the baseline and ejector wings are compared with the test data for M_0 = .15. The comparisons are very good; however, the analytical prediction for the Ejector Wing drag was found to be somewhat conservative, since an (L/D)max of ~15., vs the predicted value of 13.5, was achieved. Only qualitative predictions of roll performance were considered in the analyses. The test data more than substantiated the anticipated results for maneuvering performance.

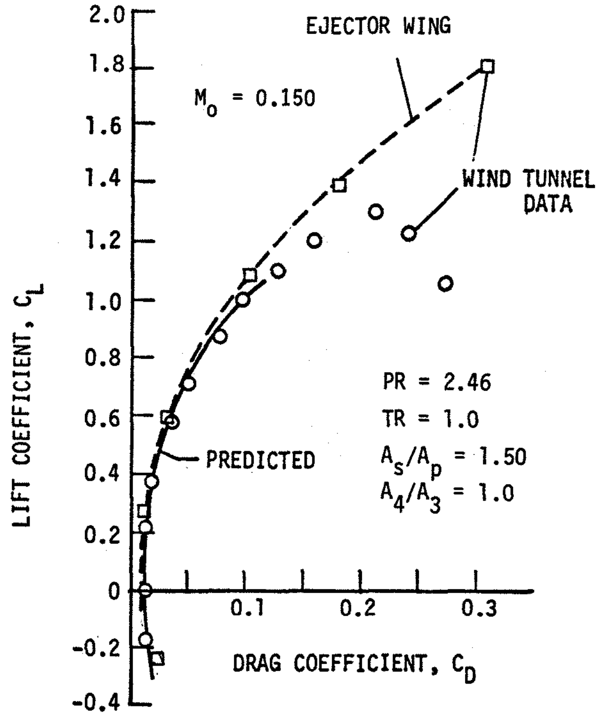

FIGURE 20. COMPARISONS OF LIFT/DRAG PERFORMANCE FOR THE BASELINE AND EJECTOR WINGS

5.0 CONCLUSIONS

The results of wind tunnel tests of the Ejector Wing configuration of this study have provided a validation of the concept which essentially takes the technology from a high risk category to a useful aeropropulsive design capability. The test results validated the analytical prediction and design procedures, as evidenced by the excellent agreement between data and predictions. The wind tunnel test model, by virtue of its three-dimensional characteristics and the realistic engine-type flow provided for the ejector operating, as well as the model's relatively large size, is representative of actual full-scale canard configurations, and is capable of achieving propulsive and aerodynamic performance benefits over a wide range of operating conditions.

Specific conclusions resulting from this study which represent notable first-time achievements in the area of integrated aeropropulsive technology are:

- An ejector thrust augmentation ratio, $\phi = 1.06$, was achieved at $M_0 = .30$ with primary flow conditions representative of actual engine bypass bleed. Augmentation performance of $\phi = 1.11$ was achieved at $M_0 = .30$ for primary flow conditions comparable to those of other previously published results - approximately 10 percent greater than the best previous efforts at that flight condition.
- Improvements in total lift coefficient of .84 over the baseline wing and .50 over the baseline with estimated "jet flap" characteristics were achieved, for the same angle of attack. The maximum angle of attack for stall was extended more than 10^o by the Ejector Wing, indicating extremely good maneuvering performance.
- The maximum lift to drag ratio (L/D)max of the Ejector Wing represented an increase of 27 percent over the baseline "clean" wing, which translates directly into a 27 percent improvement in range at the cruise condition derivable from the data base.
- Higher roll-moments were achieved by sealing off the in-board ejector bay of the four-bay configuration - another indication of extremely good maneuvering capability. No previous data on alternate partial span ejector operations in forward flight were found in the published literature.
- Static thrust augmentation ratios greater than $\phi = 1.30$ were indicated by test data obtained at $M_0 = .05$, the lowest value achievable in the wind tunnel. These results indicate excellent STOL performance for this configuration if used as a canard.

Acknowledgement

This work was performed under Air Force Contract No. F33615-79-C-3017 through the administration of the Air Force Wright Aeronautical Laboratories with support from NASA Ames Research Center, Moffett Field. The authors wish to thank D. G. Koenig and G. L. Morehouse for their technical assistance and advice during the execution of the model testing.

References

1. Keenan, J. H., Neumann, E. P., and Lustwerk, F., "An Investigation of Ejector Design by Analysis and Experiment," Journal of Applied Mechanics, pp. 299-309, September 1950.
2. Porter, J. L., and Squyers, R. A., "A Summary/Overview of Ejector Augmentor Theory and Performance," Final Report Contract No. N00014-78-C-0533, ATC Report No. R-91100/9CR-47, April 1981.
3. Hough, G. R., "Aerodynamic Performance of Jet-Flap Wings," NASA CR-1378758, 1976.
4. Haight, C. H., "Comparison of Spanwise and Chordwise Blowing for Lift Augmentation," ATC Report No. B-49300/2TR-24, 1972.
5. Hough, G. R. and Wallace, D. B., "A Simplified Method for Prouulsive-Lift System Performance Prediction," ATC Report No. B-94300/6TR-13, August 1976.
6. Haight, C. H. and Spangler, J. G., "Test Verification of a Transonic Airfoil Design Employing Active Diffusion Control," Final Report, NADC Contract No. N62269-74-C-0517, ATC Report No. B-94300/5CR-34, June 1975.
7. Hough, G. R., "An Improved Lifting-Line Approach for the Analysis of Propulsive Lift Wings," NASA CR-152147, 1978.
8. "VSD-8 Five-Component External Balance," Prepared for U. S. Army Aeronautical Research Laboratory, Report No. 2-59140/8R-50539, January 1969.